

Using the Low Concentrated Photovoltaic Module as a Preheater in an Organic Rankine Cycle

Burak Kursun 

Amasya University, Department of Mechanical Engineering, Amasya, Turkey

ABSTRACT

In concentrated photovoltaic thermal (CPVT) systems, sunlight is directly converted into electricity and during this conversion waste heat is generated on the photovoltaic module. The resulting waste heat can be used for heating the fluids. In this study, the effect of using a low concentrating photovoltaic thermal system as a pre-heater before the evaporator in the organic Rankine cycle (ORC) was investigated. Thermodynamic analyzes were performed for different solar radiation values, concentration ratio values and various photovoltaic module (PV) materials. The increase in solar radiation and concentration increased the electricity production in the photovoltaic module and the thermal efficiency of the system but led to a decrease in exergy efficiency. In the analyzes, four different PV module materials were examined and M-Si and P-Si module materials showed better performance in terms of system efficiency and electricity production.

Keywords:

Concentration ratio, Organic rankine cycle, Photovoltaic cell, Photovoltaic module, Waste heat

Article History:

Received: 2020/01/14

Accepted: 2020/01/30

Online: 2020/03/26

Correspondence to: Burak Kurşun,
Amasya University, Department of
Mechanical Engineering, Amasya,
Turkey

E-mail: burak.kursun@amasya.edu.tr;

Phone: +90 358 211 5005;

Fax: +90 358 260 0070.

INTRODUCTION

Concentrated photovoltaic thermal system (CPVT) technology has an important place among solar energy systems. In CPVT systems, sunlight is directly converted to electricity and during this conversion waste heat is generated on the photovoltaic module. The resulting waste heat can be used to heat the fluids.

Photovoltaic systems are also used in electricity and waste heat generation in steam power cycles. There is a certain number of studies on this subject in the literature. Chen et al. examined a hybrid photovoltaic / heat pump system [1]. In this study, waste heat of photovoltaic panel was utilized by using refrigerant R134a. It was observed that the performance coefficient (COP) of the system increased for high solar radiation and decreased for high flow rate. In addition, the electrical efficiency of the photovoltaic panel increased by 1.9%. Five different organic Rankine cycle (ORC) configurations, the use of photovoltaic thermal (PVT) systems for different fluid types and photovoltaic module materials have been investigated by Tourkov and Schafer [2]. As the working fluid, n-butane showed the highest performance and CdS was found to be the most compatible module mate-

rial with the configurations. Rahbar et al. combined the PVT system having different materials with a parabolic corrugated solar collector and used it as a heat source in an organic Rankine cycle [3]. R1233zd fluid was used for Rankine cycle and nano fluid (H_2O / Ag) was used for cooling of photovoltaic module. It was reported that the use of nanofluid increased the efficiency of the PVT system by 2.71%. In another study, CPVT system was used as the evaporator of an ORC [4]. R245fa was preferred as the heat transfer fluid and analyzes were performed for different solar radiation and photovoltaic module temperatures. System efficiency ranged from 9.81-11.83% depending on different parameter values. Han et al. performed thermodynamic analysis of the combination of CPVT system and concentrated solar power system [5]. In this study, it was revealed that increasing in the concentration ratio for PV module and decreasing in the exit temperature of the heat transfer fluid increased the energy and exergy efficiency. Qu et al. the use of the CPVT system with the Kalina cycle was investigated [6]. The CPVT system contributed to the LiBr-Water mixed absorption cooling system used in the cooling of the fluid exiting the turbine in the Kalina cycle. With this contribution, system efficiency increased between

2-3% and electrical module efficiency increased from 4.2% to 24% with cooling of photovoltaic module. In another study using the Kalina cycle and CPVT system, the effects of concentration ratio and module temperature on system efficiency were examined [7]. In the study, the electrical efficiency of photovoltaic module was found to be highest for 40 concentration ratio and 60 °C module temperature. Al-nimr et al. placed a photovoltaic module on the outer surface of the parabolic corrugated solar collector receiver and provided cooling of the module with the fluid in the receiver [8]. The electricity obtained from the photovoltaic module was used in hydrogen production. A thermodynamic analysis carried out for the integrated system consisting of Li-Br absorption cooling system, CPVT system and proton exchange membrane electrolyser by Akrami et al. [9]. In the study, electrical energy obtained from CPVT system was used for the production of hydrogen and the waste heat generated in the module was used for evaporation of water in the absorption cooling system. The exergy analysis revealed that the highest exergy loss was caused by the CPVT system.

In this study, unlike literature studies, CPVT system was used as preheater before evaporator in an ORC. By using the CPVT system as a pre-heater, it is aimed to increase the temperature of the heat transfer fluid before entering the evaporator, to reduce the heat load of the evaporator and to generate additional electrical energy through the photovoltaic module. The use of CPVT system as a preheater was investigated for different direct irradiation values, concentration ratios and photovoltaic module materials and energy and exergy efficiency calculations of ORC-CPVT system were performed.

MATERIAL AND METHODS

The use of the CPVT system as preheating in an ORC is shown in Fig. 1. In the ORC, the refrigerant R123 is used as the working fluid. In the system of Fig. 1, at the state 1, the fluid exits the condenser in the saturated liquid phase. In the state 2, the pressure of the fluid was increased to the evaporator pressure by the pump. The R123 fluid enters the CPVT system so that its temperature increases with the heat transfer from the solar energy and is separated from the photovoltaic module (State 3). In addition, as a result of solar radiation, electricity is produced from the photovoltaic module. The fluid becomes the superheated steam phase at the state 4. The fluid at the state 4 expands in the turbine and its pressure drops to the condenser pressure (State 5). The fluid at the state 5 becomes a saturated liquid in the state 1 by rejecting heat in the condenser and the pressure of the fluid is increased to the evaporator pressure by the pump and the cycle continues.

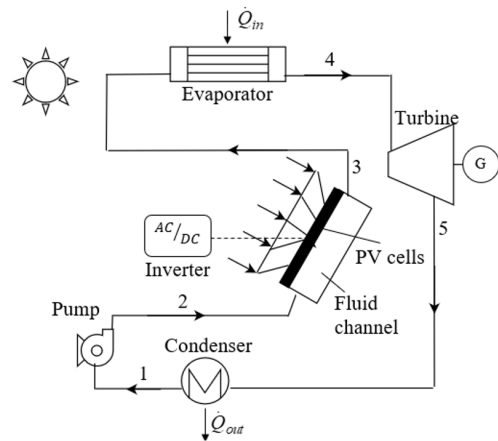


Figure 1. ORC with CPVT system

The energy and exergy calculations for the system in Fig. 1 were performed in accordance with some assumptions. All calculations were carried out for steady-state conditions. The pressure losses in the photovoltaic panel and piping line were neglected. In addition, isentropic efficiencies for pump and turbine were taken as 0.80 and 0.85, respectively [4].

The first and second laws of thermodynamics were used in the calculation of temperature, enthalpy, pressure, entropy and exergy values. The energy balance equations generated for each component given in Fig. 1 are shown in Table 1.

Table 1. Energy balance equations for each system component

Pump	$\dot{W}_p = [\dot{m}_{R123}(h_2 - h_1)]$
Evaporator	$\dot{Q}_{in} = \dot{m}_{R123}(h_4 - h_3)$
PV module	$\dot{Q}_{abs,R123} = \dot{m}_{R123}(h_3 - h_2)$
Turbine	$\dot{W}_t = [\dot{m}_{R123}(h_4 - h_5)]$
Condenser	$\dot{Q}_{out} = \dot{m}_{R123}(h_5 - h_1)$

CPVT system consists of photovoltaic module, ethylene vinyl acetate adhesives, glass cover, aluminum fluid channel and insulation (Fig. 2). The photovoltaic module converts solar rays directly into electrical energy and the temperature of the module increases during electricity generation. Some of the waste heat generated by the module is absorbed by the cold fluid and the other part is transferred to the external environment by conduction, convection and radiation heat transfer mechanisms.

The dimensions of the CPVT system and the thermal properties of the components are given in Table 2.

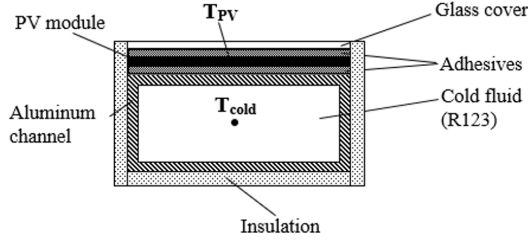


Figure 2. CPVT system structure

Table 2. CPVT system dimensions and thermal properties [6]

Material	Thickness (m)	Width (m)	Thermal conductivity (W/m.K)	Emissivity
Glass	3×10^{-3}	0.185	0.8	0.90
PV cell	3×10^{-4}	0.165	14.8	-
Adhesive	1.27×10^{-6}	0.185	0.37	-
Aluminum	4×10^{-3}	0.185	211	-
Glasswool	3×10^{-2}	0.245	0.005	0.50

The efficiency of the photovoltaic module () varies depending on the module temperature and the material of the module. The efficiency was calculated with Equation 1 given below [10],

$$\eta_{PV} = \eta_{ref} \left[1 - \beta_{ref} (T_{PV} - T_{ref}) + \gamma \log I \right] \quad (1)$$

Where, η_{ref} and β_{ref} indicates the module efficiency and the reference temperature coefficient at 25°C, respectively. T_{ref} is the reference temperature value (25°C) and I is the direct solar irradiation value. In Equation 1, the final expression in parentheses ($\gamma \log I$) can be neglected for low concentration values [10,11]. η_{ref} and β_{ref} vary according to the module material (Table 3). In actual conditions, the value β_{ref} varies slightly depending on the module temperature. However, according to the parameter values in the study, this value was considered constant since the module temperatures were close to each other [12].

Table 3. Constants for PV cell types

Material	M-Si	P-Si	Ge	CdTe
η_{ref} (%)	25	19.5	7.8	17.3
β_{ref} (1/K)	9.03×10^{-4}	9.03×10^{-4}	4.76×10^{-3}	9.26×10^{-3}

Concentrated net solar radiation is calculated by Equation 2,

$$\dot{Q}_{PV} = ICA_{PV}\eta_{opt} \quad (2)$$

In the equation C concentration ratio, APV photovoltaic module aperture area and η_{opt} optical efficiency. Optical efficiency was taken as 0.83 [4].

The part of the solar radiation transformed into electrical energy ($\dot{W}_{elec,PV}$) is calculated by Equation 3,

$$\dot{W}_{elec,PV} = \dot{Q}_{PV}\eta_{PV}\eta_{inv} \quad (3)$$

Where, η_{PV} and η_{inv} are the PV module and inverter efficiency, respectively. The inverter efficiency was taken as 0.90 [4].

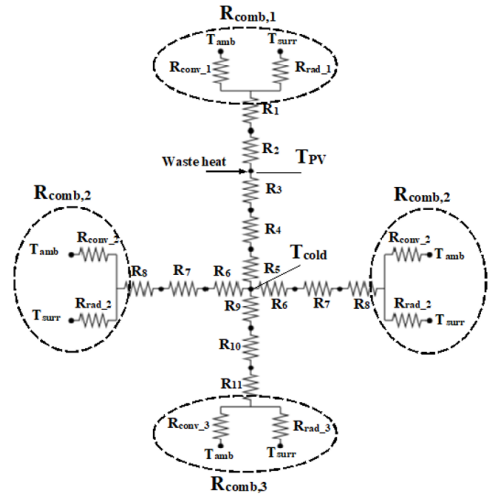
The waste heat generated by the electricity produced in the photovoltaic module is calculated by the following equation,

$$\dot{Q}_{waste} = \dot{Q}_{PV}(1 - \eta_{PV}) \quad (4)$$

While some of the waste heat is absorbed by the cold fluid in the fluid channel shown in Fig. 2, the other part is transferred from the system to the external environment as heat loss. The energy balance in these conditions can be expressed by Equation 5,

$$\dot{Q}_{waste} = \dot{Q}_{abs,cold} + \dot{Q}_{loss} \quad (5)$$

Where $\dot{Q}_{abs,cold}$ is the heat absorbed by the cold fluid and \dot{Q}_{loss} is the total heat loss to the external environment. $\dot{Q}_{abs,cold}$ and \dot{Q}_{loss} are calculated according to the thermal resistance network given in Fig. 3.



1-Glass (conduction), 2-Adhesive top (conduction), 3-Adhesive bottom (conduction) 4-Aluminum top (conduction), 5-Fluid top (convection), 6-Fluid side (convection) 7-Aluminum (conduction), 8-Insulation side (conduction), 9-Fluid bottom (convection) 10-Aluminum bottom (conduction), 11-Insulation bottom (conduction)

Figure 3. Thermal resistance network and heat transfer mechanisms

The highest temperature occurs in the photovoltaic module and some of the heat generated is transferred to the fluid and the other part is lost to the external environment. It was assumed that the temperature distribution in all la-

yers of the CPVT system was uniform. Considering the heat losses from the side surfaces of the fluid channel, heat losses from the glass surfaces, adhesives and the side surfaces of the photovoltaic module were ignored. The thermal resistances including the heat transfer mechanisms were calculated by Equation 6, 7 and 8.

$$R_{cond} = L_{thickness} / kA_{s,cond} \quad (6)$$

$$R_{conv} = 1 / hA_{s,conv} \quad (7)$$

$$R_{comb} = 1 / h_{comb}A_{s,comb} \quad T_{amb} \approx T_{surr} \quad (8)$$

In the equations, $L_{thickness}$ is the layer thickness, $A_{s,cond}$, $A_{s,conv}$ and $A_{s,comb}$ are conduction, convection and combined heat transfer surface areas, respectively. h and h_{comb} are respectively the fluid-related heat transfer coefficient and the combined heat transfer coefficient. Surrounding and ambient temperatures were taken approximately equal in terms of creating convenience in calculations [13]. The combined heat transfer coefficient including the convection and radiation effects was found by Equation 9.

$$h_{comb} = h_{conv} + h_{rad} \quad (9)$$

Here, h_{conv} and h_{rad} denote heat transfer coefficients of convection and radiation, respectively. These heat transfer coefficients were calculated by Equation 10 and 11,

$$h_{conv} = 2.8 + 3V_{wind} \quad (10)$$

$$h_{rad} = \sigma \epsilon (T_s^2 + T_{surr}^2)(T_s + T_{surr}) \quad (11)$$

Where, σ Stefan Boltzmann constant, ϵ is the emissivity and T_s surface temperature. The wind velocity was taken as 1 m / s.

The Nu number equation was used to calculate the heat transfer coefficient in the fluid region. The equation used to find the Nu number in a rectangular channel flow is given by Equation 12 [6],

$$Nu = \begin{cases} 3.66 + \frac{(0.49 + 0.02 / Pr) \left(\frac{Re Pr D_h}{L} \right)^{1.12}}{\left(1 + 0.065 \left(\frac{Re Pr D_h}{L} \right)^{0.7} \right)} & Re < 2300 \\ \frac{\left(\frac{f}{8} \right) Re Pr}{K_1(f) + K_2(Pr) \left(\frac{f}{8} \right)^{\frac{1}{2}} \left(Pr^{\frac{2}{3}} - 1 \right)} & Re \geq 2300 \end{cases} \quad (12)$$

K_1 and K_2 functions are calculated with the following equations, depending on the coefficient of friction (f) and Prandtl number (Pr),

$$K_1(f) = 1 + 3.4f \quad (13)$$

$$K_2(Pr) = 11.7 + 1.8Pr^{-\frac{1}{3}} \quad (14)$$

$$f = (1.82 \log Re - 1.64)^{-2} \quad (15)$$

Reynolds (Re) and Pr numbers are calculated by Equation 16 and 17,

$$Re = \rho V D_h / \mu \quad (16)$$

$$Pr = \mu c_p / k_{fluid} \quad (17)$$

All thermophysical properties of the fluid were determined according to the average fluid temperature. The heat transfer coefficient in the fluid channel was calculated with the following equation depending on the Nu number,

$$h = k_{fluid} Nu / D_h \quad (18)$$

Heat transfer values absorbed by the fluid and lost to the external environment were calculated by Equation 19 and 20, respectively.

$$\dot{Q}_{abs,R123} = \frac{T_{PV} - T_{cold}}{R_3 + R_4 + R_5} \quad (19)$$

$$\dot{Q}_{loss} = \frac{T_{PV} - T_{surr}}{R_1 + R_2 + R_{comb,1}} + 2 \left(\frac{T_{cold} - T_{surr}}{R_6 + R_7 + R_8 + R_{comb,2}} \right) + \left(\frac{T_{cold} - T_{surr}}{R_9 + R_{10} + R_{11} + R_{comb,3}} \right) \quad (20)$$

In the first stage of the analysis, the average fluid temperature (T_{cold}) was estimated according to the inlet temperature of the fluid. The estimated and calculated average fluid temperatures were then compared with each other. Iterations continued until the difference between the estimated and calculated mean fluid temperatures was less than 0.1°C.

Thermal efficiency of the system (η_{th}) is calculated with the equation given below,

$$\eta_{th} = \frac{\dot{W}_{net}}{\dot{Q}_{sol,CPVT} + \dot{Q}_{in}} \quad (21)$$

Where, " \dot{W}_{net} " is the net power obtained from the system, " $\dot{Q}_{sol,CPVT}$ " is the solar energy coming into the CPVT system and " \dot{Q}_{in} " is the heat input in the evaporator. These energy and heat transfer values are calculated by the following equations,

$$\dot{W}_{net} = \dot{W}_T + \dot{W}_{elec,PV} - \dot{W}_{pump} \quad (22)$$

$$\dot{Q}_{sol,CPVT} = ICA_{PV} \quad (23)$$

In the equations \dot{W}_T refers to the electrical energy obtained from the turbine, $\dot{W}_{elec,PV}$ refers to the electrical energy obtained from the CPVT system, and \dot{W}_{pump} refers to the energy input to the pump used in the ORC.

Exergy efficiency of the system (η_{ex}) was found by using Equation 24,

$$\eta_{ex} = \frac{\dot{W}_{net}}{\dot{E}_{sol,CPVT} + \dot{E}_{Q_{in}}} \quad (24)$$

The exergies of solar energy and heat input were calculated by Equation 25 [14] and Equation 26,

$$\dot{E}_{sol,CPVT} = IA_{PV}C \left(1 - \frac{4}{3} \frac{T_{amb}}{T_{sol}} + \frac{1}{3} \left(\frac{T_{amb}}{T_{sol}} \right)^4 \right) \quad (25)$$

$$\dot{E}_{Q_{in}} = \dot{Q}_{in} \left[1 - \left(\frac{T_{amb}}{T_{source}} \right) \right] \quad (26)$$

T_{sol} is the surface temperature of the sun (6000 K) and T_{source} is the temperature of the heat source (473 K). Ambient temperatures due to solar radiation were taken from an existing study in the literature [15].

Thermodynamic analysis of the CPVT system and ORC was performed using the EES commercial package program. The CPVT system and ORC simulation results were compared with the literature studies. Fig. 4 shows the comparison of the analysis results of the CPVT system for the water inlet temperature at 60 °C with the results of the literature in terms of average water and PV module temperature. The highest difference between analysis and literature results for the average water temperature and the PV module temperature were observed as 1.5% and 0.56%, respectively.

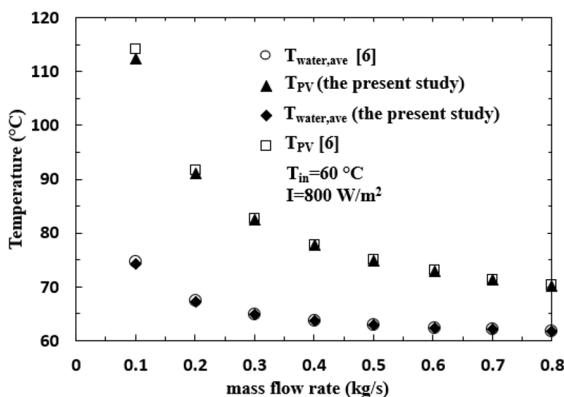


Figure 4. Validation of CPVT simulation

Validation for ORC simulation is given in Table 4. For enthalpy and entropy values, the highest deviation was 0.4% and 0.36%, respectively.

Table 4. Validation of ORC simulation with Ref. [4]

State	Temperature (°C)	Pressure (bar)	Enthalpy (kJ/kg)		Entropy (kJ/kg.K)	
			Analysis	Ref.	Analysis	Ref.
1	30	1.7904	239.1	239.6	1.135	1.1372
2	30.4	10.044	239.9	240.35	1.136	1.1377
4	90	10.044	468.2	470.48	1.7925	1.786
5	49	1.7904	444.8	445.01	1.812	1.8137

When the validation results are examined, it is seen that the analysis results are consistent with the results of the studies in the literature.

RESULTS AND DISCUSSION

In this study, the use of CPVT system as a preheater in the ORC was evaluated in terms of system efficiency and exergy. Thermodynamic analyzes were performed for different solar irradiation values, concentration ratio values and various photovoltaic module materials.

Table 4 shows the thermodynamic properties obtained at each state in the cycle for certain parameter values. The use of the CPVT system increased the temperature of the R123 fluid prior to entering the evaporator (State 3). Depending on the change in parameter values, the increase in temperature at state 3 also changed. When the CPVT system was not used, the fluid temperature was increased from 48.86 °C to 182 °C with the heat input in the evaporator. In the case of CPVT usage, the R123 temperature in the evaporator was increased from 91.22 °C to 182 °C. Thus, the heat input to the system decreased.

Table 5. Thermodynamic properties for specific parameter values ($C = 10$, $I = 964 \text{ W/m}^2$, $M\text{-Si}$, $A_{pv} = 4.95 \text{ m}^2$)

State	\dot{m} (kg/s)	T (°C)	P (kPa)	h (kJ/kg)	s (kJ/kg.K)
1	0.5	48.01	200	250.4	1.169
2	0.5	48.86	1800	251.8	1.17
3	0.5	91.22	1800	298.5	1.305
4	0.5	182	1800	509.4	1.816
5	0.5	124.4	200	124.4	1.84

Fig. 5 shows the changes in system efficiency and electricity generation as a result of different parameter changes. In Fig. 5a, efficiency and power values due to solar radiation are given. The increase in solar radiation increased the electricity production in the PV module. As a result, the

temperature of the fluid at the evaporator inlet was increased, thus the heat input required was decreased for the system. Preheating and the generation of electricity increased the thermal efficiency of the system from 12.1% to 15.5%. The condition where the radiation is zero indicates that the CPVT system is not used. On the other hand, with the use of CPVT system, it was observed that the exergy efficiency of the system decreased from 33.6% to 28.8%. This is due to the fact that the exergy of solar energy is higher than the increase in the work output obtained from the system. Since the temperature values at the state 4 and 5 were same for the both conditions, the amount of energy obtained from the turbine was constant. As can be seen from Fig. 5b, the increase in the concentration ratio increased the electrical energy obtained from the CPVT system and the temperature value at the state 3 so that the thermal efficiency ranged between 12.4-15.5%. Similar to Fig. 5a, with the increase of solar energy input, the exergy efficiency decreased from 32.6% to 28.8%. Fig. 5c shows the effects of PV module material on energy production and system efficiency. In terms of electricity generation and system efficiency, P-Si and M-Si PV module materials were found to be more convenient. This is due to the high electrical efficiency of P-Si and M-Si module materials. CdTe and Ge module materials also contributed to the generation of electricity, but the module temperatures were higher due to low electrical efficiency. The high module temperature transferred more heat energy to the fluid but decreased the electricity production and caused the thermal and exergy efficiency of the system to decrease compared to other PV materials.

CONCLUSION

When the CPVT system was used as a preheater in an ORC, the fluid temperature was increased before the evaporator and additional electricity was generated. As the heating of the fluid before the evaporator reduced the heat input to the evaporator, the thermal efficiency of the system increased. On the other hand, the use of the CPVT system has led to a decrease in the exergy efficiency as the exergy of the solar energy is higher than the increase in the work output obtained from the system.

The change of parameter values affected the amount of energy obtained and system efficiency. The increase in solar radiation and concentration ratio increased the electricity production of the PV module and thermal efficiency of the system and led to a decrease in exergy efficiency. The CPVT system was also examined for the effect of PV module material. It was observed that M-Si and P-Si module materials were more convenient in terms of system efficiency and electricity generation.

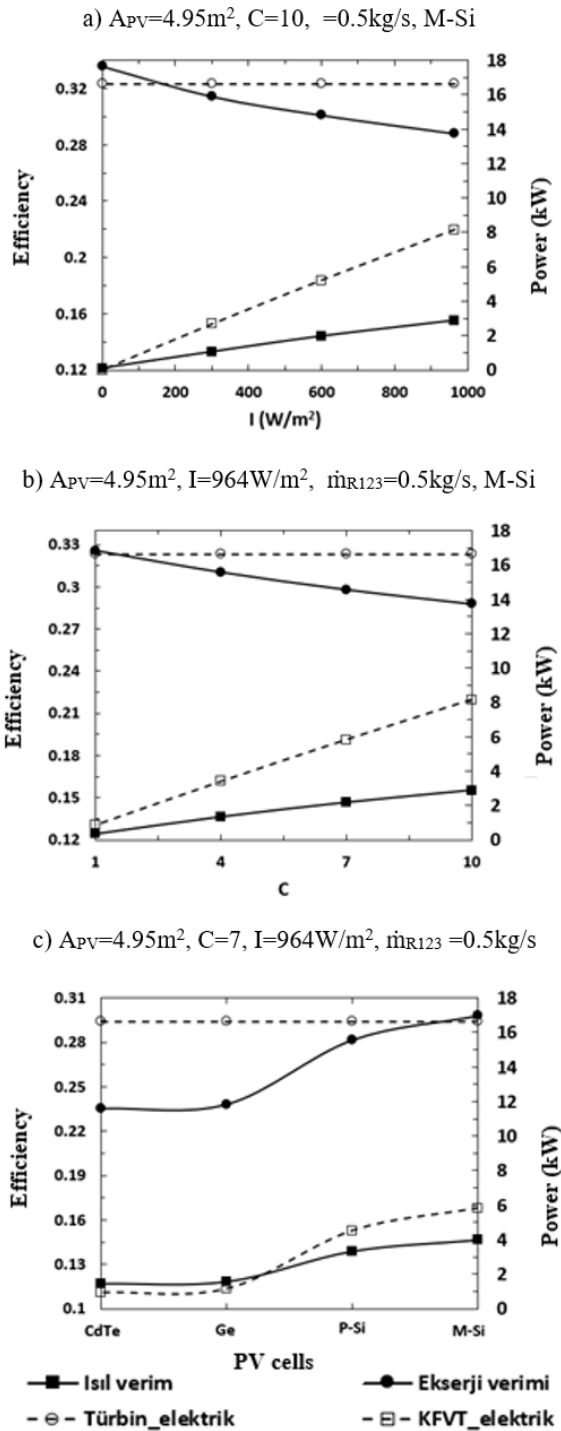


Figure 5. System efficiencies and power generations

As can be seen from the results of the analysis, the use of CPVT system as a preheater for suitable PV cell material significantly increased power production and thermal efficiency of the system.

References

1. Chen, Hongbing, Saffa B. Riffat, and Yu Fu. "Experimental study on a hybrid photovoltaic/heat pump system." *Applied Thermal Engineering* 31.17–18 (2011) 4132–4138.
2. Tourkov, Konstantin, and Laura Schaefer. "Performance evaluation of a PVT/ORC (photovoltaic thermal/organic Rankine cycle) system with optimization of the ORC and evaluation of several PV (photovoltaic) materials." *Energy* 82 (2015) 839–849.
3. Rahbar, Kiyarash, et al. "Heat recovery of nano–fluid based concentrating Photovoltaic Thermal (CPV/T) Collector with Organic Rankine Cycle." *Energy conversion and management* 179 (2019) 373–396.
4. Kosmadakis, G., D. Manolakos, and G. Papadakis. "Simulation and economic analysis of a CPV/thermal system coupled with an organic Rankine cycle for increased power generation." *Solar Energy* 85.2 (2011) 308–324.
5. Han, Xue, et al. "Parametric analysis of a hybrid solar concentrating photovoltaic/concentrating solar power (CPV/CSP) system." *Applied energy* 189 (2017) 520–533.
6. Qu, Wanjun, et al. "A concentrating photovoltaic/Kalina cycle coupled with absorption chiller." *Applied energy* 224 (2018) 481–493.
7. Qu, Wanjun, Bosheng Su, and Sanli Tang. "Thermodynamic Evaluation of a hybrid solar concentrating photovoltaic/Kalina cycle for full spectrum utilization." *Energy Procedia* 142 (2017) 597–602.
8. Moh'd A, Al-Nimr, Mohammad Bukhari, and Mansour Mansour. "A combined CPV/T and ORC solar power generation system integrated with geothermal cooling and electrolyser/fuel cell storage unit." *Energy* 133 (2017) 513–524.
9. Akrami, Ehsan, et al. "Exergy and exergoeconomic assessment of hydrogen and cooling production from concentrated PVT equipped with PEM electrolyzer and LiBr-H₂O absorption chiller." *International Journal of Hydrogen Energy* 43.2 (2018) 622–633.
10. Skoplaki, Elisa, and John A. Palyvos. "On the temperature dependence of photovoltaic module electrical performance: A review of efficiency/power correlations." *Solar energy* 83.5 (2009) 614–624.
11. Notton, Gilles, et al. "Modelling of a double-glass photovoltaic module using finite differences." *Applied thermal engineering* 25.17–18 (2005) 2854–2877.
12. Kribus, Abraham, et al. "A miniature concentrating photovoltaic and thermal system." *Energy Conversion and Management* 47.20 (2006) 3582–3590.
13. Cengel, Yunus. *Heat and mass transfer: fundamentals and applications*. McGraw–Hill Higher Education, 2014.
14. Petela, Richard. "Exergy of undiluted thermal radiation." *Solar Energy* 74.6 (2003) 469–488.
15. Jafarkazemi, Farzad, and Emad Ahmadifard. "Energetic and exergetic evaluation of flat plate solar collectors." *Renewable Energy* 56 (2013) 55–63.